Research Paper

Long non-coding RNA KRT8P41/miR-193a-3p/FUBP1 axis modulates the proliferation and invasion of chordoma cells

Hai Wen [a], Yang Fu [a], Yapeng Zhu [a], Siyue Tao [a], Xifu Shang [b], Zhongqi Li [a], Tao You [a,*], Wenzhi Zhang [a,*]

[a] Department of Orthopedics, The First Affiliated Hospital of University of Science and Technology of China (USTC), Division of Life Sciences and Medicine, University of Science and Technology of China, Hefei, Anhui Province 230036, China
[b] Department of Orthopedics, The First Affiliated Hospital of USTC, Division of Life Sciences and Medicine, University of Science and Technology of China, Hefei, Anhui Province 230001, China

A B S T R A C T

Chordomas are low-grade malignancies accounting for 1–4% of primary bone malignancies. Moreover, local recurrences increase the rate of metastasis. Our previous study identified the far upstream element (FUSE)-binding protein 1 (FUBP1) as a biomarker and potential therapeutic target for chordoma. In this study, lncRNA KRT8P41 was identified as a lncRNA positively correlated with FUBP1. In chordoma patients, higher lncRNA KRT8P41 expression was correlated with a poorer prognosis. LncRNA KRT8P41 silencing significantly inhibited chordoma cell proliferation and invasion. miR-193a was negatively correlated with lncRNA KRT8P41 and FUBP1; lncRNA KRT8P41 inhibited miR-193a expression, and miR-193a inhibited FUBP1 expression. Furthermore, miR-193a directly bound to lncRNA KRT8P41 and FUBP1 and lncRNA KRT8P41 competed with FUBP1 for miR-193a binding and relieved miR-193a-mediated FUBP1 inhibition. LncRNA KRT8P41 silencing inhibited, whereas miR-193a inhibition promoted chordoma cell proliferation and invasion; the inhibition of miR-193a attenuated the roles of lncRNA KRT8P41. Within chordoma tissues, the expression of miR-193a was decreased, and the expression of FUBP1 increased compared to normal control tissues. LncRNA KRT8P41 exhibited a positive correlation with FUBP1 and a negative correlation with miR-193a *in vivo*. Therefore, it was concluded that lncRNA KRT8P41, miR-193a-3p, and FUBP1 form a lncRNA-miRNA-mRNA axis, modulating the proliferation and invasion of chordoma cells.

© 2021 The Authors. Published by Elsevier GmbH. This is an open access article under the CC BY-NC-ND license (http://creativecommons.org/licenses/by-nc-nd/4.0/).

1. Introduction

Chordomas are clinically rare tumors originating from the embryonic remnants of the notochord or vagus chord tissue that account for 1–4% of primary bone malignancies [1]. Chordomas are low-grade malignancies prone to relapse and metastasis. The rate of metastasis can also be increased by local recurrence. [2]. Chordomas remain tolerant to radiation therapy and chemotherapy. The identification of effective biomarkers potentially providing an insight into clinical outcomes and underlying therapeutic targets is a matter of pressing clinical concern.

In our previous study, the far upstream element (FUSE)-binding protein 1 (FUBP1) was identified as a biomarker and potential therapeutic target for chordomas [3]. FUBP1 is a member of an ancient family binding to the promoter region of c-Myc proto-oncogene

and activates transcription [4,5]. The increases in FUBP1 expression were intricately linked to the tumor invading abilities into surrounding muscle tissues. Moreover, Kaplan-Meier curves have demonstrated the relationship between FUBP1 expression and the LRFS (local recurrence-free survival) of patients [3]. As per previous reports, the expression of FUBP1 was increased within lung [6], liver [7–9], stomach [10], colon [11], and pancreas [12] malignancies. Moreover, the abnormal upregulation of FUBP1 plays an oncogenic role through the deregulation of critical genes implicated in the cell cycle control and the apoptosis regulation of multiple cancers. Even though sacral chordoma patients with higher FUBP1 expression potentially predict a poorer prognosis, the mechanism involved in FUBP1 abnormal upregulation in chordoma remains obscure as of yet.

Among RNAs discovered to date, most lack protein-encoding potential and are known as non-coding RNAs (ncRNAs). There are mainly two major classes of ncRNAs based on their transcript size: short ncRNAs (mainly miRNAs) and long ncRNAs (lncRNAs) [13]. Both lncRNAs (>200 nucleotides long) and miRNAs (20-30 nucleo-

---

* Corresponding authors at: No. 1 Swan Lake Road, Shushan District, Hefei, Anhui Province 230036, China.
  E-mail addresses: youtao@ustc.edu.cn (T. You), zwzfp@163.com (W. Zhang).

tides long) could serve as tumor-suppressive or oncogenic regulators in chordoma and other malignancies [14–17]. Regarding the functional mechanism, lncRNA interacts with miRNAs and serves as endogenous competing RNAs (ceRNAs) in various pathological mechanisms. For instance, lncRNA LOC554202 regulates the proliferation and invasion capacity of chordoma cells through their influence on miR-31-mediated EZH2 expression [14]. Notably, expression profile analyses indicate deregulation in many chordoma lncRNAs and miRNAs, suggesting that the identification of more lncRNA-miRNA-mRNA axes could potentially provide novel markers in the diagnosis, prognosis, and novel treatment regimens against chordoma.

Herein, lncRNAs that positively correlated with FUBP1 were analyzed and examined for expression levels in tissue samples. Among 24 candidate lncRNAs, lncRNA KRT8P41 was the most upregulated in chordoma tissue samples. The correlation of lncRNA KRT8P41 expression with the clinical features and survival percentage in patients with chordoma was scrutinized. Moreover, the specific effects of lncRNA KRT8P41 upon the capacity of chordoma cells to proliferate and invade were also examined. Secondly, miRNAs that were negatively correlated with lncRNA KRT8P41 and FUBP1 were identified, and miR-193a was found to target lncRNA KRT8P41 and FUBP1, thereby validating the negative regulation of lncRNA KRT8P41, miR-193a, and FUBP1. The predicted miR-193a binding to lncRNA KRT8P41 and FUBP1 were examined, respectively. The dynamic effects of lncRNA KRT8P41 and miR-193a upon the expression of FUBP1 and the phenotype of chordoma cells were examined. Finally, the expression and correlation of lncRNA KRT8P41, miR-193a, and FUBP1 within tissues were examined and analyzed.

2. Materials and methods

2.1. Clinical sampling

36 chordoma tissues were harvested from patients diagnosed with sacral chordoma and underwent surgical resection in the First Affiliated Hospital of USTC (from May 2014 to May 2019). A total of 16 distant normal non-cancerous tissues were also excised from regions of a minimum distance of 3 cm away from the surgical margins as normal controls. Tissue samples were stored at $-80\,°C$ pending analysis. The follow-up was performed from May 2014 to May 2020, and the survival rate of patients was analyzed. The clinical sampling was conducted under the approval of the Ethical Committee of the First Affiliated Hospital of USTC (approval number: 2019-X(H)-025). Informed consent was obtained and signed from each patient enrolled.

2.2. Cell lines and cell culture

Two human chordoma cell lines, UCH-1 (ATCC® CRL-3217™) and JHC7 (ATCC® CRL-3267™) were procured from ATCC (Manassas, VA, USA). JHC7 cells were cultured in DMEM/F12 medium (Catalog No. 30-2006, ATCC) supplemented with 10% FBS (Invitrogen, Carlsbad, CA, USA). UCH-1 cells were cultured in a 4:1 mixture of Iscove's Modified Dulbecco's Medium (IMDM; Catalog No. 30-2005, ATCC) and RPMI-1640 medium (Invitrogen) supplemented with 10% FBS (Invitrogen) and 1% L-glutamine (Invitrogen). All the cells were cultured at 37 °C at a CO_2 saturation of 5%.

2.3. Cell transfection

LncRNA KRT8P41 silencing in target cells was achieved through the transfection of small interfering RNA targeting KRT8P41 (si-KRT8P41#1/2; GenePharma, China). miR-193a overexpression or inhibition in target cells was achieved by transfecting miR-193a mimics or miR-193a inhibitors (GenePharma). As negative controls, si-NC, mimics-NC, inhibitor-NC (GenePharma) were used, respectively. Briefly, 2×10 [5] cells/ml were plated into a 6-well plate. 24 h later, 50 nM siRNA or miRNA mimics/inhibitor were transfected into cells using 6 μl Lipofectamine 3000 (Thermo Fisher Scientific, Waltham, MA, USA) at 37C for 6 h. Then, the culture medium was replaced with a fresh culture medium. 48 h post-transfection, cells were collected for further experiments. The sequences of siRNA or miRNA mimics/inhibitor are listed in Table S1.

2.4. Polymerase chain reaction (PCR)-based analyses

The total RNA was extracted as per the aforementioned methods to detect miRNA and mRNA expression levels [18]. The expression of target genes was detected by an SYBR Green PCR Master Mix (Qiagen, Hilden, Germany) using RNU6B (for miRNA) or GAPDH (for mRNA) as an endogenous control. All data were processed using a $2^{-\Delta\Delta CT}$ method. The primers are listed in Table S1.

2.5. 3-(4, 5-dimethylthiazolyl-2)-2, 5-diphenyltetrazolium bromide (MTT) for detecting cell viability

Cells were plated into 96-well plates at a density of 3×10 [3] cells/well with a complete growth medium without antibiotics and transfected accordingly. 20 μl MTT (Sigma-Aldrich, St. Louis, MO, USA) was subsequently added to each well, and the cells were incubated for 4 h at 37 °C in 5% CO_2. After dissolving the formazan with acid isopropanol, the absorbance was determined at 490 nm on a SpectraMax Microplate® Spectrophotometer (Molecular Devices LLC, Sunnyvale, CA). The relative cell viability was calculated in each group normalized to the cell viability (as 100%) in the control group.

2.6. EdU assay for detecting DNA synthesis capacity

An EdU assay was performed using the Click-IT EdU Alexa Fluor 488 kit (Thermo Fisher, Waltham, MA, USA) as previously described [19,20]. Apollo staining and DAPI staining were performed to achieve nuclei staining. Under a fluorescence microscope, blue fluorescence indicates nuclei stained by DAPI, and the green fluorescence represents the newly synthesized DNA stained by EdU.

2.7. Colony formation assay for detecting cell proliferation

For colony formation assays, UCH1 and JHC7 cells were plated into 6-well plates at a density of 2×10 [2] cells/well 48 h after transfection. Cells were cultured in a complete growth medium without antibiotics at 37 °C for 1–2 weeks. The cells were subsequently fixed with methanol and stained with Giemsa (Sigma-Aldrich, St. Louis, MO, USA). The colony numbers were then counted.

2.8. Transwell assay for detecting cell invasion

Cell invasion was examined using a BD BioCoat™ Matrigel™ Invasion Chamber (BD; Becton-Dickinson, MA, USA). Cells were transfected and plated into the upper chambers at a density of 5×10 [4] cells/well 48 h after transfection. A serum-free medium was used in the upper chambers, and the medium supplemented with 10% FBS without antibiotics was used in the bottom chambers. After 48 h, the non-invading cells on the surface of the upper chambers were discarded with a cotton swab. Invaded cells in the bottom chambers were fixed with methanol, stained in hema-

toxylin for 15 min, and rinsed twice with distilled water. The numbers of invaded cells were then counted under a light microscope.

2.9. Immunoblotting assay for detecting protein levels

The protein levels of FUBP1 and c-Myc were examined by Immunoblotting as described before [21] using antibodies against FUBP1 (ab181111; Abcam, Cambridge, MA, USA), c-Myc (10828-1-AP; Proteintech, Rosemont, IL, USA), and GAPDH (T0004; Affinity, Cincinnati, OH, USA) (endogenous control). Proper HRP-conjugated secondary antibodies were subsequently used. The enhanced chemiluminescent (ECL) substrates (Millipore, MA, USA) were used for blot signals visualization.

2.10. Dual-luciferase reporter assay for detecting miR-193a binding to lncRNA KRT8P41 and FUBP1

The dual-luciferase reporter assay was performed following the aforementioned methods [22] to validate the predicted miR-193a binding to lncRNA KRT8P41 and FUBP1. LncRNA KRT8P41 or the 3′-untranslated region (3′UTR) of the FUBP1 gene were amplified by a PCR using a U-CH1 cell genomic DNA and cloned downstream of the Renilla luciferase open reading frame in the Renilla psi-CHECK2 vector (Promega, Madison, WI, USA). Mutations were introduced to the seed region of the miR-193a binding site in the lncRNA KRT8P41 or FUBP1 gene. The constructs were named mut-KRT8P41 or mut-FUBP1 3′UTR. miR-193a mimics/inhibitor alongside psiCHECK-2 reporter vectors (wt-/mut-KRT8P41 or wt-/mut-FUBP1 3′UTR) were subsequently co-transfected to 293 T cells. 48 h following transfection, luciferase activity was measured using a Dual-Luciferase Reporter Assay System (Promega). Values were double-normalized to firefly luciferase activity and that of the cells transfected with control plasmids.

2.11. Statistical analysis

Data from triplicate experiments were analyzed with GraphPad software and presented as a mean ± SD. The statistical significance of the results was calculated using an unpaired Student's t-test or and a one-way ANOVA test. A spearman's rank correlation coefficient analyzed the correlations of lncRNA KRT8P41, TBXT, KRT8, miR-193a, and FUBP1. Also, a log-rank test was used to analyze the survival in patients with chordoma and the data are depicted as Kaplan-Meier curves. A Cox's proportional hazard model and the multivariate analysis were used to analyze and identify the factor(s) independently affecting the patient prognosis. P values of less than 0.05 were deemed statistically significant.

3. Results

3.1. Selection of lncRNAs related to FUBP1 in chordoma

To identify lncRNAs positively correlated with FUBP1, GSE98021 and divided cases in GSE98021 were downloaded into the high FUBP1 group and the low FUBP1 group using the median value of FUBP1 expression as a cut-off. The correlation of FUBP1 and the differentially expressed genes in chordoma tissues was analyzed. A total of 24 lncRNAs (ABCC13, ALDOAP2, CROCCP3, FAM138B, GAPDHP62, GEMIN8P4, GUSBP5, JMJD1C-AS1, KRT8P41, LOXL1-AS1, MNX1-AS1, NME2P1, OR10D1P, OR1F2P, PFN1P2, PGAM1P4, PLAC4, PYY2, RPS10P7, RPS2P32, SCAND2P, TCF4-AS1, TPI1P2, TPM3P9) were subsequently found to be significantly positively correlated with FUBP1 (Fig. 1A). The expression of these 24 lncRNAs was verified in a small sample size; in 5 cases chordoma tissues, lncRNA KRT8P41 expression was the most upregulated

when compared with the paired non-cancerous tissues (Fig. 1B). lncRNA KRT8P41 expression was subsequently confirmed in tissue specimens (non-cancerous specimens n = 16, chordoma specimens n = 36). Consistently, lncRNA KRT8P41 was dramatically increased within chordoma tissue specimens compared to the controls (Fig. 1C). Moreover, the chordoma biomarkers, T-Box Transcription Factor T (TBXT) and keratin 8 (KRT8) levels were significantly increased in tumor tissues (Fig. 1D and E) and positively correlated with lncRNA KRT8P41 levels in chordoma tumor tissues (Fig. 1F). To evaluate the sensitivity and specificity of lncRNA KRT8P41 expression as a diagnostic biomarker, lncRNA KRT8P41 expression was used to calculate the area under the receiver operating characteristic (ROC) curve (AUC). The area under the curve (AUC) is 0.837 (Fig. 1D), indicating that lncRNA KRT8P41 expression acts as a diagnostic biomarker for chordoma with satisfactory efficiency. Moreover, patients with chordoma were divided into a high lncRNA KRT8P41 and a low lncRNA KRT8P41 group. Also, the correlation of lncRNA KRT8P41 expression with the clinical features of chordoma patients was analyzed. Table 1 showed that higher lncRNA KRT8P41 expression was closely linked to advanced tumor stage (P = 0.023) and surrounding muscle invasion (P = 0.008). Moreover, univariate and multivariate analyses by Cox's proportional hazard model indicated that lncRNA KRT8P41 expression presented a substantial risk to patients with chordoma (HR (hazard ratio), 3.680; 95% CI (confidence interval), 1.231–11.000; P = 0.020) (Table 2.). The survival percentage of chordoma patients with high or low lncRNA KRT8P41 expression was analyzed using a log-rank test, as depicted by the Kaplan-Meier curves in Fig. 1E, patients with lower lncRNA KRT8P41 expression displayed a higher survival percentage. These data indicate that lncRNA KRT8P41 expression is upregulated in chordoma and potentially serves as an oncogenic lncRNA in chordoma.

3.2. Effects of lncRNA KRT8P41 on chordoma cell malignant behaviors

To validate the specific effects of lncRNA KRT8P41 on chordoma cell phenotype, the silencing of lncRNA KRT8P41 was achieved within U-CH1 and JHC7 by transfecting si-KRT8P41#1/2 in two chordoma cell lines. The transfection efficiency was verified using a real-time qPCR. The test showed that si-KRT8P41#1 had a better silencing effect and was selected for further experiments (Fig. 2A). In both chordoma cell lines, lncRNA KRT8P41 silencing significantly inhibited cell viability (Fig. 2B-C), DNA synthesis capacity (Fig. 2D), colony formation capacity (Fig. 2E), and cell invasion (Fig. 2F). These data indicate that lncRNA KRT8P41 silencing represses the malignant traits of chordoma cells.

3.3. Selection of miRNA negatively correlated to FUBP1 and lncRNA KRT8P41

To investigate the underlying mechanism, the correlation between FUBP1 and lncRNA KRT8P41was further confirmed in U-CH1 and JHC7 cells. In both cell lines, lncRNA KRT8P41 silencing significantly decreased the FUBP1 protein levels (Fig. 3A-B). Since miR-NAs have been reported to mediate the crosstalk between lncRNAs and mRNAs, next, using the online tool miRCode (http://www.mircode.org/), the present study identified miRNAs that could target FUBP1 and lncRNA KRT8P41; two sets of miRNAs intersected at the following miRNAs: miR-193/193b/193a-3p, miR-192/215, miR-183, miR-338/338-3p, miR-216b/216b-5p, miR-29abcd, and miR-216a (Fig. 3C). miRNAs differentially expressed in chordoma and non-cancerous tissues were subsequently analyzed based on GSE56183, and these two steps intersected at miR-193a (Fig. 3D). To validate the correlation of miR-193a with lncRNA KRT8P41 and FUBP1, miR-193a overexpression or inhibition was achieved in U-CH1 and JHC7 cells by transfecting miR-193a mimics/in-
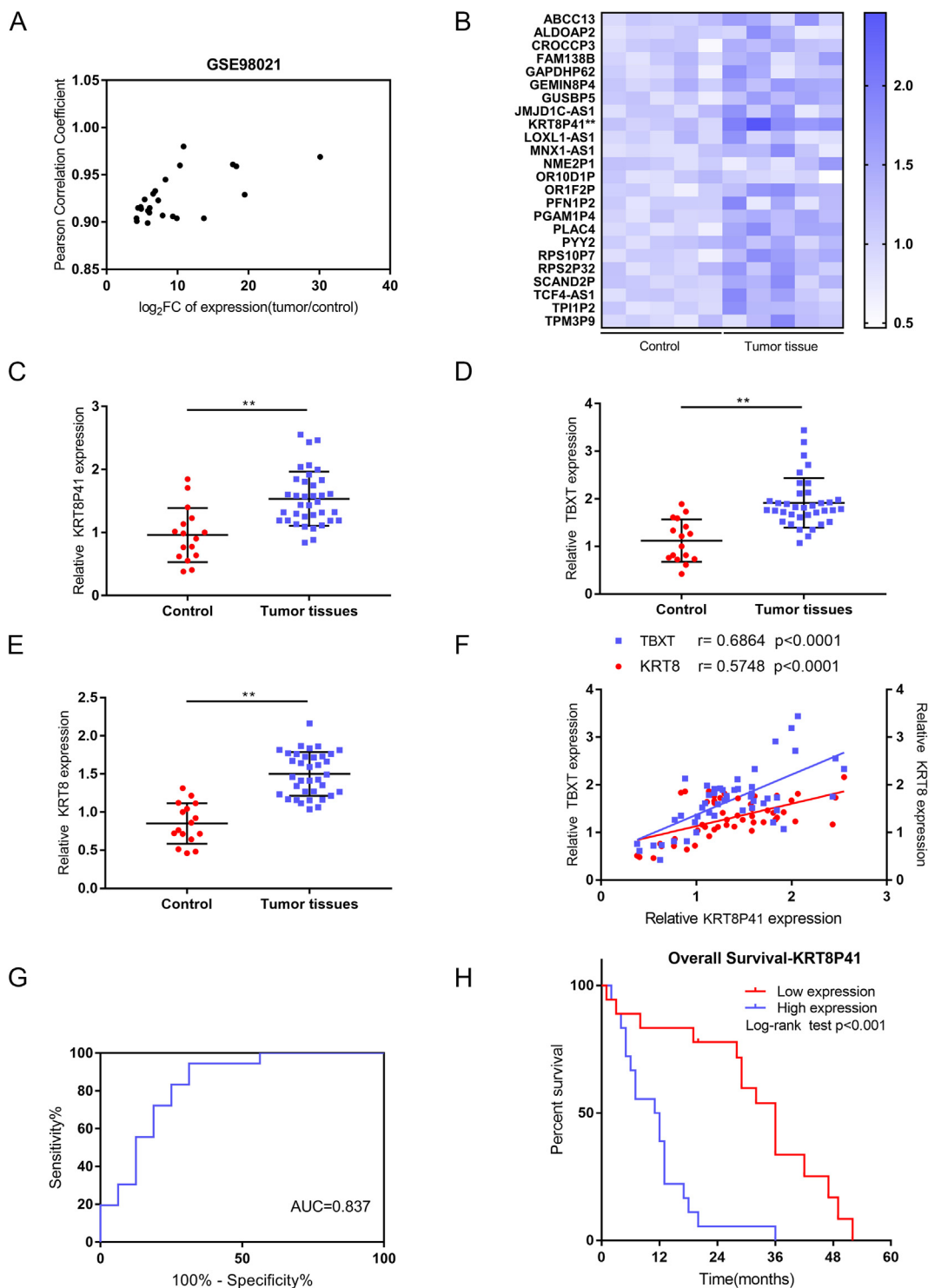
Fig. 1. Selection of lncRNAs related to FUBP1 in chordoma (A) Cases in GSE98021 were divided into high FUBP1 group and low FUBP1 group using the median value of FUBP1 expression as cut-off; a total of 24 lncRNAs (ABCC13, ALDOAP2, CROCCP3, FAM138B, GAPDHP62, GEMIN8P4, GUSBP5, JMJD1C-AS1, KRT8P41, LOXL1-AS1, MNX1-AS1, NME2P1, OR10D1P, OR1F2P, PFN1P2, PGAM1P4, PLAC4, PYY2, RPS10P7, RPS2P32, SCAND2P, TCF4-AS1, TPI1P2, TPM3P9) were found to be significantly positively correlated with FUBP1. (B) The expression of these 24 lncRNAs was determined in a total of 5 paired chordoma and non-cancerous tissue samples using real-time qPCR. (C–E) The expression of lncRNA KRT8P41, TBXT and KRT8 was determined in 16 non-cancerous and 36 chordoma tissue samples using real-time qPCR. (F) The correlations of lncRNA KRT8P41between TBXT or KRT8 in tissue samples were analyzed using Spearman's rank correlation coefficient analysis. (G) The area under the receiver operating characteristic (ROC) curve (AUC) was calculated using the expression levels of lncRNA KRT8P41. (H) The survival percentage of chordoma patients with high or low lncRNA KRT8P41 expression was analyzed using a log-rank test and shown as Kaplan-Meier curves. **$P < 0.01$.

hibitor, as confirmed by real-time qPCR (Fig. 3E). In both cell lines, lncRNA KRT8P41 silencing also regulated miR-193a expression (Fig. 3F). Similarly, in both cell lines, miR-193a negatively regu-lated the protein levels of FUBP1 (Fig. 3G-H). These data indicate that lncRNA KRT8P41 negatively regulates miR-193a, and miR-193a negatively regulates FUBP1.

Table 1

Association between KRT8P41 expression and the clinicopathologic characteristics of patients with sacral chordoma.

Variables		KRT8P41 expression		p value
		High	Low	
Age (years)	<50	7	8	0.735
	≥50	11	10	
Gender	female	6	9	0.310
	male	12	9	
Tumor location	Above S3	12	9	0.310
	S3 and below	6	9	
Tumor size (cm)	< 5	5	11	0.044
	≥5	13	7	
Tumor grade	High	14	9	0.083
	Low	4	9	
Tumor stage *	I	3	11	0.023
	II	11	6	
	III	4	1	
Surrounding muscle invasion	No	5	13	0.008
	Yes	13	5	
Type of resection	EA	8	12	0.180
	EI	10	6	

EI, Enneking inappropriate; EA, Enneking appropriate. *, using the Fisher's exact test.

Table 2

Univariate and multivariate analysis for factors related to overall survival using the COX proportional hazard model.

Variable		Univariate analysis			Multivariate analysis		
		p value	HR	95%CI	p value	HR	95%CI
Age (years)	<50 vs ≥ 50	0.664	1.167	0.582–2.341			
Gender	female vs male	0.269	0.666	0.324–1.369			
Tumor location	Above S3 vs S3 and below	0.825	1.084	0.532–2.208			
Tumor size (cm)	<5 vs ≥ 5	0.133	0.550	0.253–1.200			
Tumor grade	High vs Low	0.358	0.712	0.345–1.468			
Tumor stage	I vs II+III	0.004	0.314	0.141–0.697	0.320	0.627	0.249–1.574
Surrounding muscle invasion	No vs Yes	0.016	0.397	0.187–0.843	0.512	0.721	0.272–1.915
Type of resection	EA vs EI	0.052	0.486	0.235–1.007	0.090	0.490	0.215–1.117
KRT8P41 expression	High vs Low	<0.001	5.039	2.200–11.542	0.020	3.680	1.231–11.000

EI, Enneking inappropriate; EA, Enneking appropriate.

3.4. miR-193a binds to lncRNA KRT8P41 and FUBP1 3′UTR

Regarding the putative miR-193a binding lncRNA KRT8P41 and FUBP1 3′UTR, respectively, the study performed a dual-luciferase reporter assay. The predicted miR-193a binding site in lncRNA KRT8P41 or the 3′UTR of FUBP1 and the structures of wt/mut-KRT8P41 and wt/mut-FUBP1 3′UTR luciferase reporter plasmids are illustrated in Fig. 4A, and C. These luciferase reporter plasmids in 293 T cells were transfected with miR-193a mimics or miR-193a inhibitor the luciferase activity was examined. Fig. 4B and D showed that the overexpression of miR-193a was dramatically repressed, whereas the inhibition of miR-193a enhanced the luciferase activity of both wt-KRT8P41 and wt-FUBP1 3′UTR. However, when co-transfected with mutant plasmids, miR-193a overexpression or inhibition failed to alter the luciferase activity.

To further substantiate the confirmation on the binding of miR-193a to lncRNA KRT8P41 and the 3′UTR of FUBP1, respectively, further RIP assays were performed using AGO2 or IgG antibody [23]. In AGO2 antibody immunoprecipitates, the levels of miR-193a, lncRNA KRT8P41, and FUBP1 were significantly higher than those in IgG antibody immunoprecipitates (Fig. 4E). Moreover, in miR-193a-overexpressing cells, higher levels of lncRNA KRT8P41 and FUBP1 were observed in the anti-AGO2 immunoprecipitates compared to the mimics-NC group. The levels of lncRNA KRT8P41 were also higher than FUBP1 (Fig. 4F). It was therefore concluded that miR-193a could bind to lncRNA KRT8P41 and the 3′UTR of FUBP1, respectively.

3.5. LncRNA KRT8P41/miR-193a axis modulates chordoma cell aggressiveness through FUBP1

After confirming miR-193a binding to lncRNA KRT8P41 and the 3′UTR of FUBP1, U-CH1, and JHC7 cells were subsequently co-transfected with a miR-193a inhibitor and si-KRT8P41 and were examined for chordoma cell phenotype. LncRNA KRT8P41 silencing significantly repressed, whereas miR-193a inhibition promoted cell viability (Fig. 5A-B) and cell invasion (Fig. 5C); the inhibition of miR-193a attenuated the roles of lncRNA KRT8P41 knockdown in chordoma cell phenotype (Fig. 5A-C). Regarding the molecular mechanism, the knockdown of lncRNA KRT8P41 inhibited, whereas the inhibition of miR-193a promoted FUBP1 and c-Myc protein contents. Similarly, the inhibition of miR-193a attenuated the effects of lncRNA KRT8P41 silencing on FUBP1 and c-Myc (Fig. 5D and E). It was concluded that lncRNA KRT8P41 relieves miR-193a-mediated FUBP1 inhibition by acting as a ceRNA, promoting chordoma cell aggressiveness.

3.6. Expression and correlation of lncRNA KRT8P41, miR-193a, and FUBP1 within tissues

Finally, miR-193a and FUBP1 expression were examined in 16 non-cancerous and 36 chordoma tissue samples using a real-time qPCR; Fig. 6A-B showed that the expression of miR-193a was dramatically decreased, whereas the expression of FUBP1 was
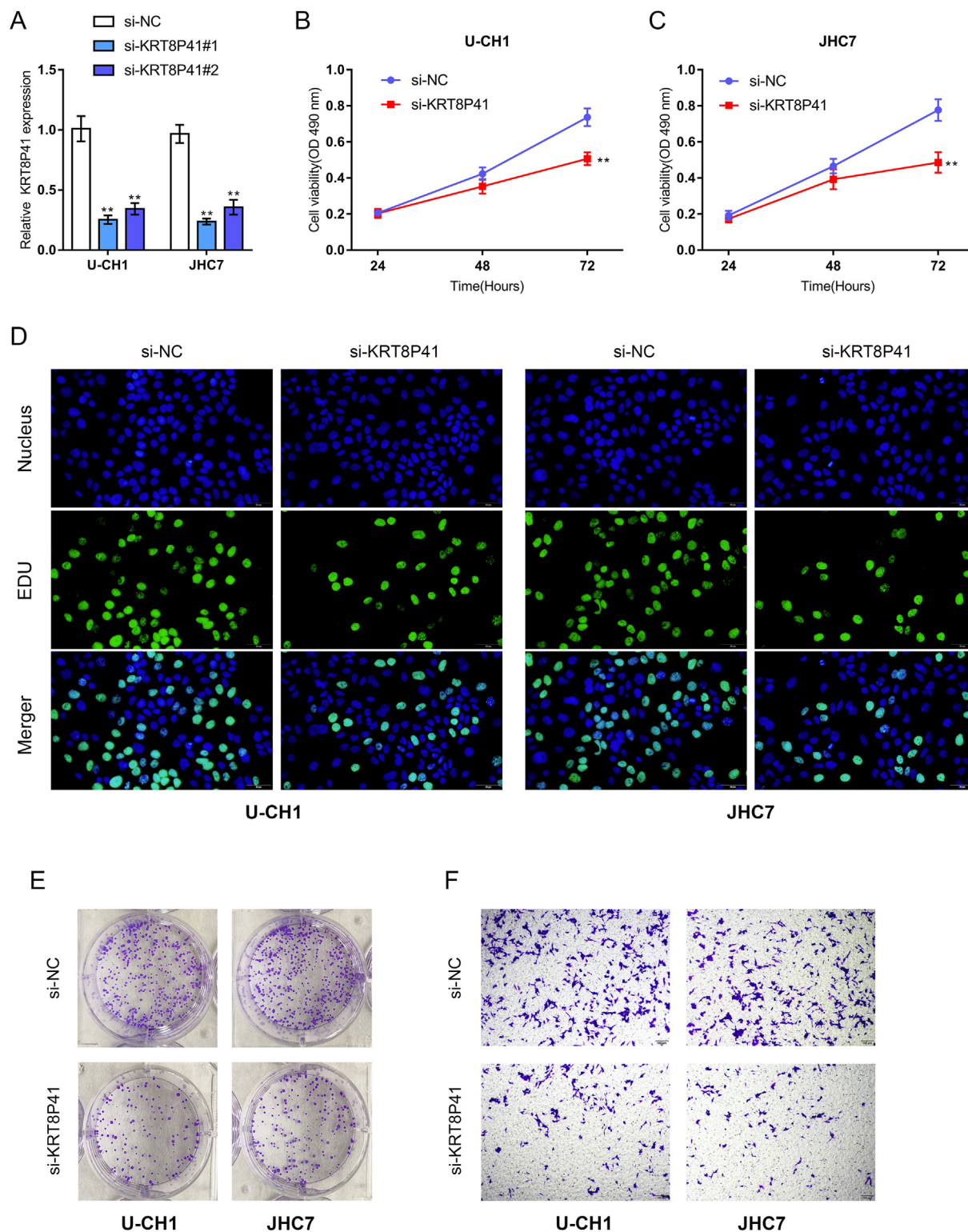
Fig. 2. Effects of lncRNA KRT8P41 on chordoma cell malignant behaviors (A) The silencing of lncRNA KRT8P41 in two chordoma cell lines, U-CH1 and JHC7, was achieved by transfecting si-KRT8P41#1/2. The transfection efficiency was verified using real-time qPCR, and si-KRT8P41#1 was used in further experiments because of better efficiency. Then, these two chordoma cell lines were transfected with si-KRT8P41 and examined for (B and C) cell viability by MTT assay; (D) DNA synthesis capacity by EdU assay; (E) colony formation capacity by Colony formation assay; (F) cell invasion by Transwell assay. **$P < 0.01$.

increased within chordoma tissue samples compared to the controls. In tissue samples, lncRNA KRT8P41 and FUBP1 were positively correlated, whereas lncRNA KRT8P41 and miR-193a were negatively correlated (Fig. 6C).

4. Discussion

Herein, the study demonstrated lncRNA KRT8P41 as a lncRNA positively correlated with FUBP1. In chordoma patients, a higher
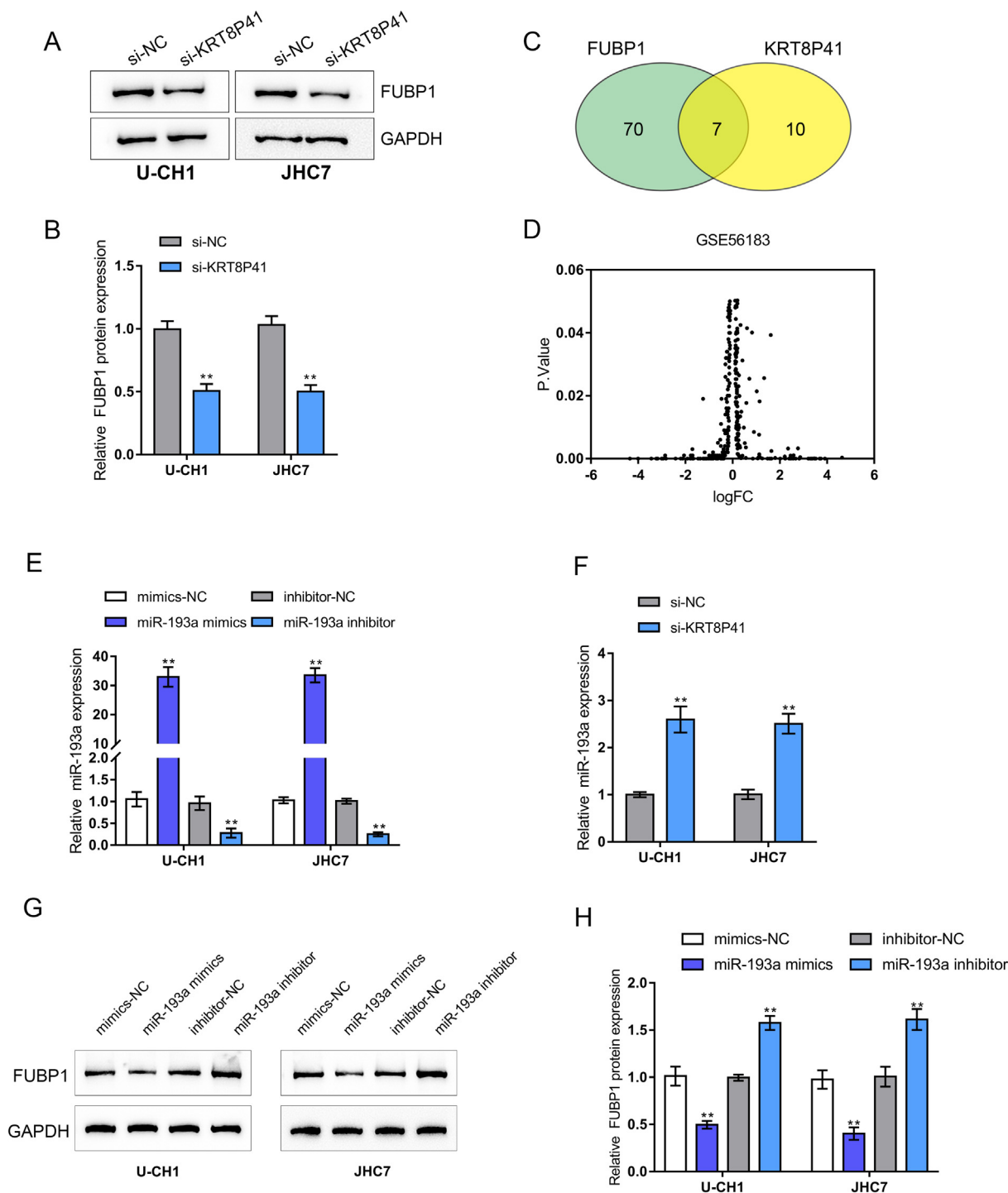
Fig. 3. Selection of miRNA negatively correlated to FUBP1 and lncRNA KRT8P41 (A-B) U-CH1 and JHC7 cells were transfected with si-KRT8P41 and examined for FUBP1 protein levels using Immunoblotting. (C) Online tool miRCode (http://www.mircode.org/) was used to predict miRNAs that could target FUBP1 and lncRNA KRT8P41, and the following miRNAs were found: miR-193/193b/193a-3p, miR-192/215, miR-183, miR-338/338-3p, miR-216b/216b-5p, miR-29abcd, and miR-216a. (D) miRNAs differentially expressed in chordoma and non-cancerous tissues according to GSE56183 were shown. These two steps intersected at miR-193a. (E) miR-193a overexpression or inhibition was achieved in U-CH1, and JHC7 cells by transfecting miR-193a mimics/inhibitor. The transfection efficiency was verified using real-time qPCR. (F) U-CH1 and JHC7 cells were transfected with si-KRT8P41 and examined for miR-193a expression using real-time qPCR. (G and H) U-CH1 and JHC7 cells were transfected with miR-193a mimics/inhibitor and examined for FUBP1 protein levels using Immunoblotting. **$P < 0.01$.

lncRNA KRT8P41 expression was correlated with a poorer prognosis. LncRNA KRT8P41 silencing significantly inhibited chordoma cell proliferation and invasion. Also, miR-193a was negatively correlated with lncRNA KRT8P41 and FUBP1; lncRNA KRT8P41 inhibited miR-193a expression, and miR-193a inhibited FUBP1 expression. miR-193a is directly bound to lncRNA KRT8P41 and

FUBP1. Moreover, lncRNA KRT8P41 competed with FUBP1 for miR-193a binding and alleviated miR-193a-mediated FUBP1 inhibition. LncRNA KRT8P41 silencing inhibited, whereas miR-193a inhibition promoted chordoma cell proliferation and invasion. The inhibition of miR-193a attenuated the roles of lncRNA KRT8P41. Within chordoma tissues, the expression of miR-193a
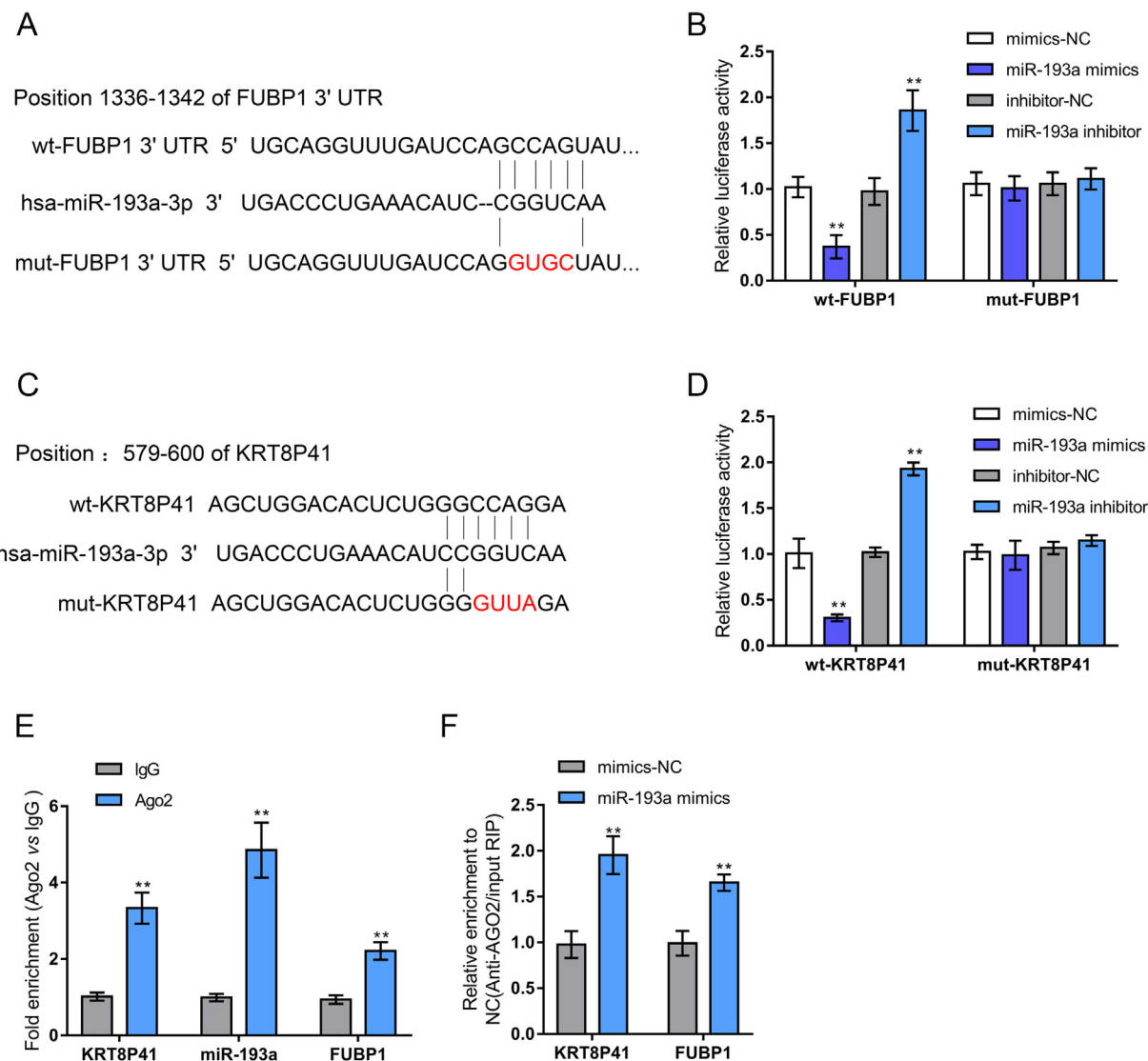
Fig. 4. miR-193a binds to lncRNA KRT8P41 and the 3′UTR of FUBP1 (A and C) The schematic diagrams showing the predicted miR-193a binding site in lncRNA KRT8P41 or the 3′UTR of FUBP1 and the structures of wt/mut-KRT8P41 and wt/mut-FUBP1 3′UTR luciferase reporter plasmids. (B and D) Luciferase reporter plasmids were co-transfected in 293 T cells with miR-193a mimics/inhibitor. The luciferase activity was determined. (E-F) RIP assays were performed to confirm miR-193a binding to lncRNA KRT8P41 and FUBP1 3′-UTR using IgG or AGO2 antibody. The levels of lncRNA KRT8P41, miR-193a, and FUBP1 in precipitated IgG or AGO2 proteins were examined using real-time PCR. **$P < 0.01$.

was decreased, and the expression of FUBP1 was increased compared to normal control tissues. In tissue samples, lncRNA KRT8P41 exhibited a positive correlation with FUBP1 and a negative correlation with miR-193a.

FUBP1 has been reported to bind the c-Myc promoter, thereby activating c-Myc transcription and expression [4]. FUBP1 has been identified as a prognostic biomarker in nasopharyngeal carcinoma, and FUBP1 expression was positively correlated with c-Myc. Moreover, FUBP1 elicits c-Myc expression, enhancing cancer stem cell-like characteristics within nasopharyngeal carcinoma [24]. Our previous study also demonstrated FUBP1 as a biomarker implicated in tumor progression and poor prognosis in chordoma patients. Similarly, FUBP1 expression in chordoma also correlated with c-Myc expression [3]. In this study, a significantly positive correlation was established between lncRNA KRT8P41 and FUBP1, suggesting that lncRNA KRT8P41 also potentially acts as a biomarker in the prognosis of chordoma. In addition, the diagnostic biomarkers of chordoma, Brachyury (TBXT) [25] and KRT8 [26] expression also positively correlated with the lncRNA KRT8P41

levels in the chordoma tissues. Based on clinical data collected, higher lncRNA KRT8P41 expression was related to bigger-sized tumors, advanced tumor grading, and surrounding muscle invasion. Furthermore, patients with higher lncRNA KRT8P41 expression displayed a more deficient survival percentage. With an AUC of 0.837, lncRNA KRT8P41 could also potentially serve as an effective prognostic biomarker in chordoma.

Although the prognostic role of lncRNAs in chordoma has been reported, only a few studies have demonstrated the functional role of lncRNAs in chordoma. For instance, lncRNA LINC00662 relieves miR-16-5p-induced RNF144B inhibition by acting as a ceRNA, affecting proliferation, colony formation, invasion, migration, EMT, and glycolysis in chordoma cells and tumor growth *in vivo* [27]. Another lncRNA, LOC554202, has been reported to recruit EZH2 and regulate miR-31 expression, modulating the invasive and proliferative capacity of chordoma cells [14]. As mentioned above, FUBP1 activates the expression of proto-oncogene c-Myc [4], exerting crucial effects on cell-cycle control, metabolism, apoptosis, differentiation, cellular adhesion, and carcinogenesis [28,29].
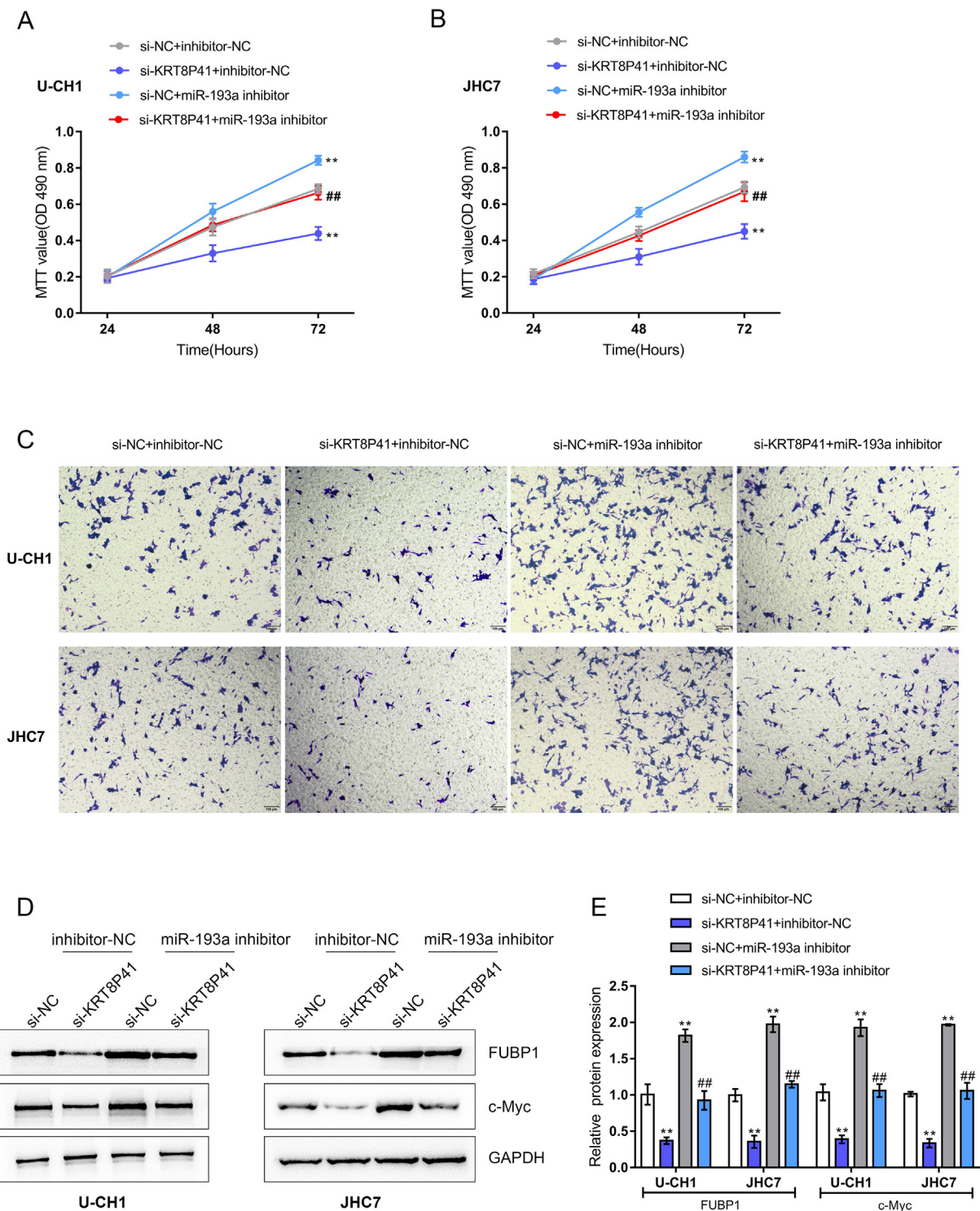
Fig. 5. LncRNA KRT8P41/miR-193a axis modulates chordoma cell aggressiveness through FUBP1 U-CH1 and JHC7 cells were co-transfected with miR-193a inhibitor and si-KRT8P41 and examined for (A and B) cell viability by MTT assay; (C) cell invasion by Transwell assay; (D and E) the protein levels of FUBP1 and c-Myc by Immunoblotting. $^{**}P < 0.01$, compared with the control group; $^{##}P < 0.01$, compared with the si-NC + miR-193a inhibitor group.

Considering the positive correlation between lncRNA KRT8P41 and FUBP1, it is speculated that lncRNA KRT8P41 could potentially affect chordoma cell proliferation and invasion. As predicted, lncRNA KRT8P41 silencing inhibited chordoma cell viability, DNA synthesis, colony formation, and cell invasion. Thus, abnormally upregulated lncRNA KRT8P41 in chordoma cells could promote cancer cell aggressiveness.

To further investigate the molecular mechanism underlying the positive correlation between lncRNA KRT8P41 and FUBP1, online tools were used to search for candidate miRNAs potentially targeting lncRNA KRT8P41 and FUBP1, respectively. miR-193a was subsequently found. By competing with FUBP1 for miR-193a binding, lncRNA KRT8P41 could counteract a miR-193a-mediated FUBP1 inhibition. Also, miR-193a belongs to the miR-193 family
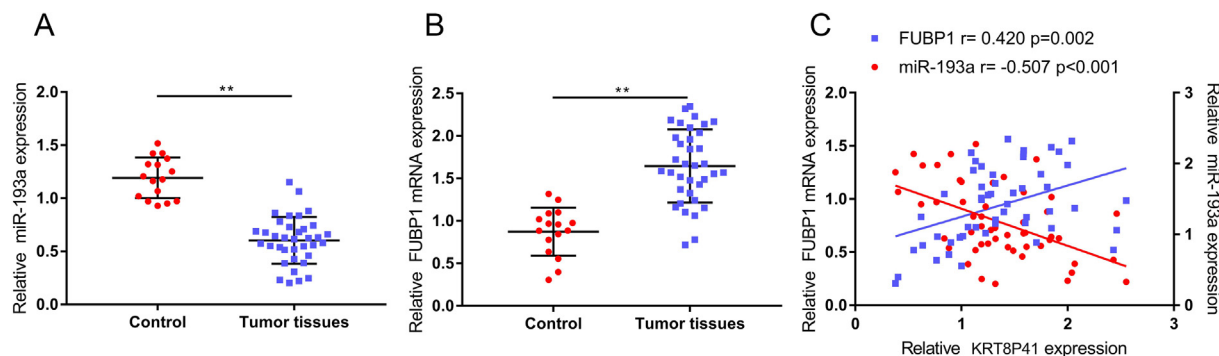
Fig. 6. Expression and correlation of lncRNA KRT8P41, miR-193a, and FUBP1 in tissue samples (A and B) The expression levels of miR-193a and FUBP1 were examined in 16 non-cancerous and 36 chordoma tissue samples using real-time qPCR. **$P < 0.01$. (C) The correlations of lncRNA KRT8P41, miR-193a, and FUBP1 in tissue samples were analyzed using Spearman's rank correlation coefficient analysis.

[30]. As per previous reports, miR-193a-3p exerts a tumor-suppressive effect on both liquid and solid tumors [31]. miR-193a-3p shows to be under-expressed within ulcerative colitis-neoplasia, and miR-193a-3p loss promotes carcinogenesis through the upregulation of IL17RD [32]. Moreover, miR-193-3p serves as downstream targets of lncRNA NEAT1 in colorectal cancer [33] and lncRNA UCA1 in non-small cell lung cancer, impacting the proliferative and invasive ability of cancer cells. Herein, miR-193a-3p inhibition also promoted chordoma cell proliferation and invasion. Furthermore, miR-193a-3p inhibition significantly attenuated the tumor-suppressive roles of lncRNA KRT8P41 knockdown, indicating that lncRNA KRT8P41 serves its functions through miR-193a-3p.

In conclusion, lncRNA KRT8P41, miR-193a-3p, and FUBP1 form a lncRNA-miRNA-mRNA axis modulating the proliferation and invasion of chordoma cells. Although the correlation between KRT8P41 and chordoma biological markers has been tested in the present study, the direct interaction remains to be investigated. Thus, the molecular mechanism should be further explored in the future study.

5. Data availability statement

The data supporting the findings of this study are available from the author upon reasonable request.

CRediT authorship contribution statement

Hai Wen: Writing - original draft, Investigation. **Yang Fu:** . **Yapeng Zhu:** Investigation, Visualization. **Siyue Tao:** . **Xifu Shang:** . **Zhongqi Li:** Investigation, Visualization. **Tao You:** Writing - review & editing, Validation. **Wenzhi Zhang:** Writing - review & editing, Validation.

Declaration of Competing Interest

The authors declare that they have no known competing financial interests or personal relationships that could have appeared to influence the work reported in this paper.

Acknowledgment

Appendix A. Supplementary data

Supplementary data to this article can be found online at https://doi.org/10.1016/j.jbo.2021.100392.

References

[1] B.P. Walcott, B.V. Nahed, A. Mohyeldin, J.-V. Coumans, K.T. Kahle, M.J. Ferreira, Chordoma: current concepts, management, and future directions, Lancet Oncol. 13 (2) (2012) e69–e76.

[2] B.J. Jian, O.G. Bloch, I. Yang, S.J. Han, D. Aranda, A.T. Parsa, A comprehensive analysis of intracranial chordoma and survival: a systematic review, Br. J. Neurosurg. 25 (4) (2011) 446–453.

[3] H. Wen, H. Ma, P. Li, J. Zheng, Y. Yu, G. Lv, Expression of far upstream element-binding protein 1 correlates with c-Myc expression in sacral chordomas and is associated with tumor progression and poor prognosis, Biochem. Biophys. Res. Commun. 491 (4) (2017) 1047–1054.

[4] R. Duncan, L. Bazar, G. Michelotti, T. Tomonaga, H. Krutzsch, M. Avigan, D. Levens, A sequence-specific, single-strand binding protein activates the far upstream element of c-myc and defines a new DNA-binding motif, Genes Dev. 8 (4) (1994) 465–480.

[5] M.I. Avigan, B. Strober, D. Levens, A far upstream element stimulates c-myc expression in undifferentiated leukemia cells, J. Biol. Chem. 265 (30) (1990) 18538–18545.

[6] S. Singer, M. Malz, E. Herpel, A. Warth, M. Bissinger, M. Keith, T. Muley, M. Meister, H. Hoffmann, R. Penzel, G. Gdynia, V. Ehemann, P.A. Schnabel, R. Kuner, P. Huber, P. Schirmacher, K. Breuhahn, Coordinated expression of stathmin family members by far upstream sequence element-binding protein-1 increases motility in non-small cell lung cancer, Cancer Res. 69 (6) (2009) 2234–2243.

[7] J. Ma, M. Chen, S.K. Xia, W. Shu, Y. Guo, Y.H. Wang, Y. Xu, X.M. Bai, L. Zhang, H. Zhang, et al., Prostaglandin E2 promotes liver cancer cell growth by the upregulation of FUSE-binding protein 1 expression, Int. J. Oncol. 42 (2013) 1093–1104.

[8] U. Rabenhorst, R. Beinoraviciute-Kellner, M.-L. Brezniceanu, S. Joos, F. Devens, P. Lichter, R.J. Rieker, J. Trojan, H.-J. Chung, D.L. Levens, M. Zörnig, Overexpression of the far upstream element binding protein 1 in hepatocellular carcinoma is required for tumor growth, Hepatology 50 (4) (2009) 1121–1129.

[9] M. Malz, M. Bovet, J. Samarin, U. Rabenhorst, C. Sticht, M. Bissinger, S. Roessler, J.L. Bermejo, M. Renner, D.F. Calvisi, S. Singer, M. Ganzinger, A. Weber, N. Gretz, M. Zörnig, P. Schirmacher, K. Breuhahn, Overexpression of far upstream element (FUSE) binding protein (FBP)-interacting repressor (FIR) supports growth of hepatocellular carcinoma, Hepatology 60 (4) (2014) 1241–1250.

[10] F. Zhang, Q. Tian, Y. Wang, Far upstream element-binding protein 1 (FUBP1) is overexpressed in human gastric cancer tissue compared to non-cancerous tissue, Onkologie 36 (2013) 650–655.

[11] M.Y. Jia, Y.J. Wang, Far upstream element-binding protein 1(FUBP1) expression differs between human colorectal cancer and non-cancerous tissue, Neoplasma 61 (2014) 533–540.

[12] P. Fan, J. Ma, X. Jin, Far upstream element-binding protein 1 is up-regulated in pancreatic cancer and modulates immune response by increasing programmed death ligand 1, Biochem. Biophys. Res. Commun. 505 (3) (2018) 830–836.

[13] J. Sana, P. Faltejskova, M. Svoboda, O. Slaby, Novel classes of non-coding RNAs and cancer, J. Transl. Med. 10 (2012) 103.

[14] X. Ma, S. Qi, Z. Duan, H. Liao, B. Yang, W. Wang, J. Tan, Q. Li, X. Xia, Long non-coding RNA LOC554202 modulates chordoma cell proliferation and invasion by recruiting EZH2 and regulating miR-31 expression, Cell Prolif. 50 (6) (2017) e12388, https://doi.org/10.1111/cpr.12388.

[15] H. Chen, K. Zhang, J. Lu, G. Wu, H. Yang, K. Chen, Comprehensive analysis of mRNA-lncRNA co-expression profile revealing crucial role of imprinted gene cluster DLK1-MEG3 in chordoma, Oncotarget 8 (68) (2017) 112623–112635.
[16] Z. Duan, E. Choy, G.P. Nielsen, A. Rosenberg, J. Iafrate, C. Yang, J. Schwab, H. Mankin, R. Xavier, F.J. Hornicek, Differential expression of microRNA (miRNA) in chordoma reveals a role for miRNA-1 in Met expression, J. Orthop. Res. 28 (6) (2010) 746–752.
[17] J. Ma, W. Chen, K. Wang, K. Tian, Q. Li, T. Zhao, L. Zhang, L. Wang, Z. Wu, J. Zhang, Identification of the different roles and potential mechanisms of T isoforms in the tumor recurrence and cell cycle of chordomas, Onco Targets Ther. 12 (2019) 11777–11791.
[18] Y. Liu, Y. Wang, X. He, S. Zhang, K. Wang, H. Wu, L. Chen, LncRNA TINCR/miR-31-5p/C/EBP-alpha feedback loop modulates the adipogenic differentiation process in human adipose tissue-derived mesenchymal stem cells, Stem Cell Res. 32 (2018) 35–42.
[19] Z. Liu, C. Dou, B. Yao, M. Xu, L. Ding, Y. Wang, Y. Jia, Q. Li, H. Zhang, K. Tu, T. Song, Q. Liu, Ftx non coding RNA-derived miR-545 promotes cell proliferation by targeting RIG-I in hepatocellular carcinoma, Oncotarget 7 (18) (2016) 25350–25365.
[20] K. Tu, Z. Liu, B. Yao, S. Han, W. Yang, MicroRNA-519a promotes tumor growth by targeting PTEN/PI3K/AKT signaling in hepatocellular carcinoma, Int. J. Oncol. 48 (2016) 965–974.
[21] H. Liu, H. Deng, Y. Zhao, C. Li, Y. Liang, LncRNA XIST/miR-34a axis modulates the cell proliferation and tumor growth of thyroid cancer through MET-PI3K-AKT signaling, J. Exp. Clin. Cancer Res. 37 (2018) 279.
[22] L. Donato, C. Scimone, C. Rinaldi, P. Aragona, S. Briuglia, A. D'Ascola, R. D'Angelo, A. Sidoti, Stargardt Phenotype Associated With Two ELOVL4 Promoter Variants and ELOVL4 Downregulation: New Possible Perspective to Etiopathogenesis?, Invest Ophthalmol. Vis. Sci. 59 (2) (2018) 843, https://doi.org/10.1167/iovs.17-22962.
[23] V.M. King, G.M. Borchert, MicroRNA Expression: Protein Participants in MicroRNA Regulation, Methods Mol. Biol. 1617 (2017) 27–37.
[24] Z.H. Liu, J.L. Hu, J.Z. Liang, A.J. Zhou, M.Z. Li, S.M. Yan, X. Zhang, S. Gao, L. Chen, Q. Zhong, et al., Far upstream element-binding protein 1 is a prognostic biomarker and promotes nasopharyngeal carcinoma progression, Cell Death Dis 6 (2015), e1920.
[25] V. Barresi, A. Ieni, G. Branca, G. Tuccari, Brachyury: a diagnostic marker for the differential diagnosis of chordoma and hemangioblastoma versus neoplastic histological mimickers, Dis. Markers 2014 (2014) 1–7.
[26] S. Gulluoglu, O. Turksoy, A. Kuskucu, U. Ture, O.F. Bayrak, The molecular aspects of chordoma, Neurosurg. Rev. 39 (2) (2016) 185–196.
[27] C.B. Wang, Y. Wang, J.J. Wang, X.L. Guo, LINC00662 triggers malignant progression of chordoma by the activation of RNF144B via targeting miR-16-5p, Eur. Rev. Med. Pharmacol. Sci. 24 (2020) 1007–1022.
[28] Z.E. Stine, Z.E. Walton, B.J. Altman, A.L. Hsieh, C.V. Dang, MYC, Metabolism, and Cancer, Cancer Discov 5 (10) (2015) 1024–1039.
[29] D.M. Miller, S.D. Thomas, A. Islam, D. Muench, K. Sedoris, c-Myc and cancer metabolism, Clin. Cancer Res. 18 (20) (2012) 5546–5553.
[30] M. Khordadmehr, R. Shahbazi, S. Sadreddini, B. Baradaran, miR-193: A new weapon against cancer, J. Cell. Physiol. 234 (10) (2019) 16861–16872.
[31] I. Grossi, A. Salvi, E. Abeni, E. Marchina, G. De Petro, Biological Function of MicroRNA193a-3p in Health and Disease, Int J Genomics 2017 (2017) 1–13.
[32] J. Pekow, K. Meckel, U. Dougherty, Y. Huang, X. Chen, A. Almoghrabi, R. Mustafi, F. Ayaloglu-Butun, Z. Deng, H.I. Haider, J. Hart, D.T. Rubin, J.H. Kwon, M. Bissonnette, miR-193a-3p is a Key Tumor Suppressor in Ulcerative Colitis-Associated Colon Cancer and Promotes Carcinogenesis through Upregulation of IL17RD, Clin. Cancer Res. 23 (17) (2017) 5281–5291.
[33] H.-M. Yu, C. Wang, Z. Yuan, G.-L. Chen, T. Ye, B.-W. Yang, LncRNA NEAT1 promotes the tumorigenesis of colorectal cancer by sponging miR-193a-3p, Cell Prolif. 52 (1) (2019) e12526, https://doi.org/10.1111/cpr.2019.52.issue-110.1111/cpr.12526.

Further reading

[34] W. Nie, H.-J. Ge, X.-Q. Yang, X. Sun, H. Huang, X. Tao, W.-S. Chen, B. Li, LncRNA-UCA1 exerts oncogenic functions in non-small cell lung cancer by targeting miR-193a-3p, Cancer Lett. 371 (1) (2016) 99–106.